2008

Attachment of molecular hydrogen to an isolated boron cation: an infrared and ab initio study

Viktoras Dryza
University Of Melbourne

Berwyck L. J Poad
University of Wollongong, bpoad@uow.edu.au

Evan J. Bieske
University Of Melbourne

Attachment of molecular hydrogen to an isolated boron cation: an infrared and ab initio study

Abstract

Structural properties of the $B^+–H_2$ electrostatic complex are investigated through its rotationally resolved infrared spectrum in the H–H stretch region (3905–3975 cm^{-1}). The spectrum, which was obtained by monitoring B^+ photofragments while the IR wavelength was scanned, is consistent with the complex having a T-shaped structure and a vibrationally averaged intermolecular separation of 2.26 Å, which decreases by 0.04 Å when the H_2 subunit is vibrationally excited. The H–H stretch transition of $B^+–H_2$ is red-shifted by 220.6 ± 1.5 cm^{-1} from that of the free H_2 molecule, much more than for other dihydrogen complexes with comparable binding energies. Properties of $B^+–H_2$ and the related $Li^+–H_2$, $Na^+–H_2$, and $Al^+–H_2$ complexes are explored through ab initio calculations at the MP2/aug-cc-pVTZ level. The unusually large red-shift for $B^+–H_2$ is explained as due to electron donation from the H_2 σ_g bonding orbital to the unoccupied $2p_z$ orbital on the B^+ ion.

Keywords

infrared, ab, attachment, molecular, initio, hydrogen, study, isolated, boron, cation, GeoQUEST

Disciplines

Life Sciences | Physical Sciences and Mathematics | Social and Behavioral Sciences

Publication Details

Dryza, V., Poad, B. L. J. & Bieske, E. J. (2008). Attachment of molecular hydrogen to an isolated boron cation: An infrared and ab initio study. Journal of the American Chemical Society, 130 (39), 12986-12991.

J|A|C|S
ARTICLES

Published on Web 09/04/2008

Attachment of Molecular Hydrogen to an Isolated Boron Cation: An Infrared and ab initio Study

Viktoras Dryza, Berwyck L. J. Poad, and Evan J. Bieske*

School of Chemistry, The University of Melbourne, Victoria, Australia 3010

Received March 17, 2008; E-mail: evanjb@unimelb.edu.au

Abstract: Structural properties of the B^+-H_2 electrostatic complex are investigated through its rotationally resolved infrared spectrum in the H−H stretch region (3905−3975 cm^{-1}). The spectrum, which was obtained by monitoring B^+ photofragments while the IR wavelength was scanned, is consistent with the complex having a T-shaped structure and a vibrationally averaged intermolecular separation of 2.26 Å, which decreases by 0.04 Å when the H_2 subunit is vibrationally excited. The H−H stretch transition of B^+-H_2 is red-shifted by 220.6 ± 1.5 cm^{-1} from that of the free H_2 molecule, much more than for other dihydrogen complexes with comparable binding energies. Properties of B^+-H_2 and the related Li^+-H_2, Na^+-H_2, and Al^+-H_2 complexes are explored through ab initio calculations at the MP2/aug-cc-pVTZ level. The unusually large red-shift for B^+-H_2 is explained as due to electron donation from the H_2 σ_g bonding orbital to the unoccupied $2p_z$ orbital on the B^+ ion.

1. Introduction

One obstacle to the use of hydrogen as a clean fuel is the lack of suitable storage materials. Viable storage media must possess high capacity, favorable uptake and release kinetics,[1] and, to achieve a large weight percentage of hydrogen, contain primarily lighter elements.[2] Additionally, to maximize storage capacity, the material's microstructure should be optimized for high porosity and surface area. Among a variety of promising materials, which include metal hydrides,[2] complex hydrides,[3] metalorganic frameworks,[4] and zeolites,[5] are several boron-containing substances including boron nitride nanotubes[6,7] and boron-doped fullerenes and nanostructures.[8,9] Recent density functional and quantum Monte Carlo calculations on boron-doped carbon nanostructures suggest that H_2 attaches nondissociatively at the boron sites, with typical binding energies suitable for reversible hydrogen storage near standard conditions (i.e., 5−15 kcal/mol) and a barrierless hydrogen adsorption process, simplifying the uptake and release kinetics.[8] The existence of an empty, localized boron p_z orbital was found to be essential for nondissociative H_2 adsorption. X-ray photoelectron spectra and reactivity studies of boron doped fullerenes indicate a partial positive charge on the boron atoms, consistent with the computational results.[10−13]

There are several challenges associated with applying computational approaches to modeling hydrogen storage materials. Perhaps most importantly, the relatively weak interaction between dihydrogen and the bulk medium requires an accurate, reliable description. To this end, calculations are often calibrated by considering smaller subsystems in which a hydrogen molecule is attached to just a single atom or small molecule.[5,14,15] Once buttressed by agreement between experimental and theoretical data for the isolated M^+-H_2 complex (intermolecular bond energies, intermolecular separations, and vibrational frequencies), the theoretical approach can be used confidently for more realistic hydrogen storage materials. The current study's aim is to facilitate this process for boron-containing systems by providing quantitative structural data for the isolated B^+-H_2 complex in the gas phase. The use of infrared spectroscopy to probe the structures of ionic complexes and clusters in the gas phase is well-established,[16,17] although high resolution spectra, from which quantitative structural data can be derived, remain scarce.[18]

Previous theoretical and experimental studies of $[BH_2]^+$ suggest that it possesses the two stable configurations shown

(1) Schlapbach, L.; Zuttel, A. *Nature* **2001**, *414*, 353–358.
(2) Grochala, W.; Edwards, P. P. *Chem. Rev.* **2004**, *104*, 1283–1315.
(3) Orimo, S.; Nakamori, Y.; Eliseo, J.; Zuttel, A.; Jensen, C. *Chem. Rev.* **2007**, *107*, 4111–4132.
(4) Mulder, F. M.; Dingemans, T. J.; Wagemaker, M.; Kearley, G. J. *Chem. Phys.* **2005**, *317*, 113–118.
(5) Vitillo, J. G.; Damin, A.; Zecchina, A.; Ricchiardi, G. *J. Chem. Phys.* **2005**, *122*, 114311/1–114311/10.
(6) Fakioglu, E.; Yurum, Y.; Veziroglu, N. T. *Int. J. Hydrogen Energy* **2004**, *29*, 1371–1376.
(7) Tang, C.; Bando, Y.; Ding, X.; Qi, S.; Golberg, D. *J. Am. Chem. Soc.* **2002**, *124*, 14550–14551.
(8) Kim, Y.-H.; Zhao, Y.; Williamson, A.; Heben, M. J.; Zhang, S. B. *Phys. Rev. Lett.* **2006**, *96*, 016102.
(9) Liu, Y.; Brown, C. M.; Blackburn, J. L.; Neumann, D. A.; Gennett, T.; Simpson, L.; Parilla, P.; Dillion, A. C.; Heben, M. J. *J. Alloys Compd.* **2007**, *446*, 368–372.
(10) Guo, T.; Jin, C.; Smalley, R. E. *J. Phys. Chem.* **1991**, *95*, 4948–4950.
(11) Muhr, H.-J.; Nesper, R.; Schnyder, B.; Kotz, R. *Chem. Phys. Lett.* **1996**, *249*, 399–405.
(12) Zou, Y. J.; Zhang, X. W.; Ll, Y. L.; Wang, B.; Yan, H. *J. Mater. Sci.* **2002**, *37*, 1043–1047.
(13) Xie, R.-H.; Bryant, G. W.; Zhao, J.; Smith, V. H. J.; Carlo, A. D.; Pecchia, A. *Phys. Rev. Lett.* **2003**, *90*, 206602.
(14) Lochan, R. C.; Head-Gordon, M. *Phys. Chem. Chem. Phys.* **2006**, *8*, 1357–1370.
(15) Hübner, O.; Klopper, W. *J. Phys. Chem. A* **2007**, *111*, 2426–2433.
(16) Duncan, M. A. *Int. J. Mass Spectrom.* **2000**, *200*, 545–569.
(17) Lisy, J. M. *J. Chem. Phys.* **2006**, *125*, 132302.
(18) Bieske, E. J.; Dopfer, O. *Chem. Rev.* **2000**, *100*, 3963–3998.
(19) Nichols, J.; Gutowski, M.; Cole, S. J.; Simons, J. *J. Phys. Chem.* **1992**, *96*, 644–650.

10.1021/ja8018302 CCC: $40.75

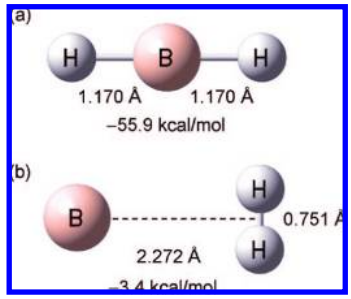

Figure 1. Stable forms of the $[BH_2]^+$ system: (a) the minimum energy BH_2^+ covalent structure and (b) the weakly bound B^+-H_2 complex. Energies are with respect to the $B^+ + H_2$ limit. Structural and energetic parameters are taken from ref 21.

in Figure 1.[19−22] The lower energy BH_2^+ form (Figure 1a) features covalent B−H bonds, sp hybridization on the B^+ atom, and a linear, $D_{\infty h}$ structure. In comparison, the electrostatic B^+-H_2 complex (Figure 1b), which is predicted to lie 53 kcal/mol higher in energy, has a C_{2v} structure, a relatively long, weak intermolecular bond, and an almost undistorted H_2 subunit.[21] This T-shaped configuration for the B^+-H_2 complex is favored by the electrostatic interaction between the B^+ cation and the H_2 quadrupole moment. The binding energy of the electrostatic complex with respect to the $B^+ + H_2$ fragments was measured by Bowers and co-workers as 3.8 kcal/mol through clustering equilibrium measurements,[20] in good agreement with the calculations of Sharp and Gellene (3.4 kcal/mol).[21] Conversion from the B^+-H_2 complex to the covalent BH_2^+ form is predicted to entail surmounting a considerable 57 kcal/mol barrier.[21] Intriguingly, transformation from the electrostatic form to the covalent form is expedited in larger $B^+-(H_2)_n$ clusters with a drastic lowering of the barrier to 3.4 kcal/mol for the $n = 3$ cluster.[20,21]

Here we present and analyze the first rotationally resolved infrared spectrum of the B^+-H_2 complex in order to characterize the bond between a hydrogen molecule and an isolated B^+ cation and as a step toward understanding the interaction between H_2 and bulk boron-containing materials. Prior to this study, neither the electrostatic B^+-H_2 complex nor the covalent BH_2^+ molecule had been observed spectroscopically.

The current investigation complements earlier spectroscopic studies of similar complexes, including Li^+-H_2, Li^+-D_2, and Al^+-H_2, using photodissociation spectroscopy in the H−H or D−D stretch region.[23−25] The cohesive forces in these metal ion−dihydrogen clusters originate predominantly from electrostatic charge−quadrupole interactions and charge-induced-dipole induction interactions. The spectra, which are obtained by monitoring charged photofragments, generally feature rotationally resolved substructure and provide fundamental structural and vibrational data, including the intermolecular bond length, the frequency of the H_2 stretch vibration, and an estimate for the intermolecular stretch frequency.

One significant issue we wish to explore is the correlation between a cluster's binding energy (D_0) and the red-shift in the H_2 stretch frequency ($\Delta\nu_{HH}$). This is an important point given that in solid media the dihydrogen binding energy is often estimated from the magnitude of $\Delta\nu_{HH}$; generally, large dissociation energies are associated with large $\Delta\nu_{HH}$ values.[5] Vitillo, Damin, Zecchina, and Ricchiardi compiled experimental and theoretical data for dihydrogen interacting with a range of cations, finding a roughly linear correlation between D_0 and $\Delta\nu_{HH}$ data for 25 different weakly to moderately bound complexes ($D_0 \leq 8$ kcal/mol).[5] Whereas the Li^+-H_2 and Na^+-H_2 data fit the general linear trend, the B^+-H_2 point lies clear from the other data. Here we confirm experimentally the rather large vibrational red-shift predicted computationally for B^+-H_2 and investigate its origin through ab initio calculations for B^+-H_2 and similar dihydrogen complexes that have recently been characterized spectroscopically (Li^+-H_2, Na^+-H_2, and Al^+-H_2). Ultimately, we find that the large vibrational red-shift for B^+-H_2 is associated with significant electron donation from the H_2 σ_g bonding orbital to the cation's empty $2p_z$ orbital which, in the case of B^+, lies energetically close by.

2. Experimental and Computational Approaches

The infrared (IR) spectrum of $^{11}B^+-H_2$ in the H−H stretch region was obtained using infrared photodissociation (IRPD) spectroscopy, whereby $^{11}B^+$ photofragments were monitored while the IR wavelength was scanned. The IRPD process entails absorption of an IR photon (having an appropriate frequency to excite the H−H stretch vibrational mode), followed by migration of the vibrational energy into the weak intermolecular bond causing its rupture and liberation of a detectable B^+ fragment. The IRPD scheme's efficacy for obtaining a rotationally resolved infrared spectrum of B^+-H_2 relies on two factors. First, photoexcitation of the H−H stretch vibrational mode must provide sufficient energy to sever the $B^+\cdots H_2$ bond. This condition is likely satisfied as the B^+-H_2 dissociation energy has been measured as ~1330 cm^{-1},[20] considerably less than the H−H stretch frequency, which is predicted to be only ~5% lower than that of the free H_2 molecule (4161 cm^{-1}).[21] Second, the dissociation process must be relatively slow so that individual rovibrational lines are not drastically affected by lifetime broadening, thereby obscuring rotational structure in the spectrum. This implies that the coupling between the H−H stretch vibrational mode and the dissociation coordinate (i.e., the intermolecular bond) should be relatively weak. This has proven to be the case for Li^+-H_2 and Al^+-H_2 dihydrogen complexes which exhibit rotationally resolved IRPD spectra in the H−H stretch region.[23,25]

The IRPD strategy was implemented using a tandem mass spectrometer coupled to a pulsed, tunable IR source (Continuum Mirage 3000 optical parametric oscillator, bandwidth ~0.017 cm^{-1}). The B^+-H_2 complexes were generated in a supersonic expansion of H_2 (8 bar) passed over a laser-ablated BN rod. The translating/rotating rod was irradiated with the fundamental (1064 nm, 7 mJ/pulse), doubled (532 nm, 3 mJ/pulse), and quadrupled (266 nm, 1 mJ/pulse) output of a pulsed Nd:YAG laser running at 20 Hz. The B^+-H_2 ions were mass-selected by a quadrupole mass filter and deflected through 90° by a quadrupole bender into an octopole ion guide where they were overlapped by the counter-propagating IR pulse. Resulting B^+ photofragments were mass-selected by a second quadrupole mass filter and detected using a microchannel plate coupled to a scintillator and a photomultiplier tube. We estimate that each IR pulse irradiated ~100 B^+-H_2 ions. Calibration of the infrared wavelength was achieved using the methods described in refs 24 and 25.

(20) Kemper, P. R.; Bushnell, J. E.; Weis, P.; Bowers, M. T. *J. Am. Chem. Soc.* **1998**, *120*, 7577.
(21) Sharp, S. B.; Gellene, G. I. *J. Am. Chem. Soc.* **1998**, *120*, 7585.
(22) Rasul, G.; Prakash, G. K. S.; Olah, G. A. *J. Phys. Chem. A* **2000**, *104*, 2284–2286.
(23) Emmeluth, C.; Poad, B. L. J.; Thompson, C. D.; Weddle, G. H.; Bieske, E. J. *J. Chem. Phys.* **2007**, *126*, 204309.
(24) Thompson, C.; Emmeluth, C.; Poad, B.; Weddle, G.; Bieske, E. *J. Chem. Phys.* **2006**, *125*, 044310−5.
(25) Emmeluth, C.; Poad, B. L. J.; Thompson, C. D.; Weddle, G. H.; Bieske, E. J.; Buchachenko, A. A.; Grinev, T. A.; Kłos, J. *J. Chem. Phys.* **2007**, *127*, 164310.

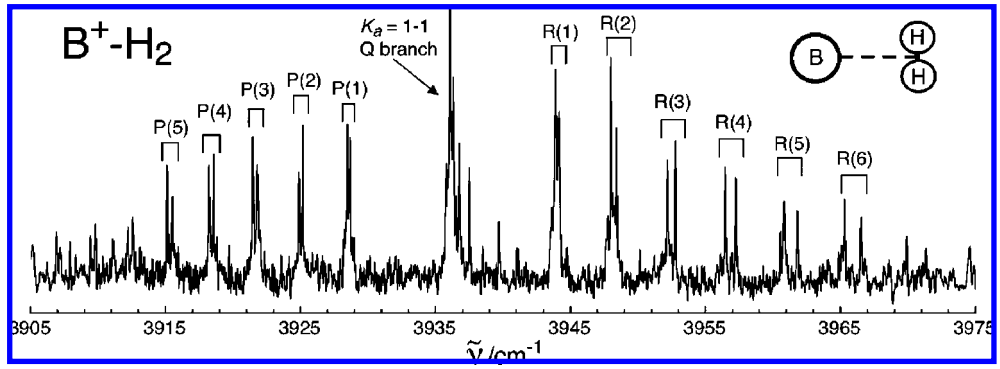

Figure 2. Infrared spectrum of B^+-H_2 in the H−H stretch region obtained by monitoring B^+ photofragments while the infrared wavelength was scanned. The $K_a = 1-1$ transitions are labeled.

Ab initio calculations at the MP2/aug-cc-pVTZ level[26] were performed to determine optimum geometries, vibrational frequencies, and dissociation energies for the B^+-H_2, Li^+-H_2, Na^+-H_2, and Al^+-H_2 complexes. The calculations were performed using the Gaussian 03 suite of programs.[27] For comparison with experimental values, the calculated H−H stretch vibrational frequencies were scaled by the factor required to reconcile the calculated and experimental frequencies for the free H_2 molecule (0.921). Harmonic zero-point energies were accounted for in the determination of cluster dissociation energies. The effect of basis set superposition error (BSSE) on the calculated binding energies was ignored.

3. Results

The infrared spectrum of B^+-H_2 over the 3905−3975 cm^{-1} range is shown in Figure 2. The observed band is associated with excitation of the H−H stretch vibrational mode and has the unmistakeable form expected for an *A*-type transition of a T-shaped B^+-H_2 complex (Figure 1b); the observed $K_a = 1-1$ transitions follow $\Delta K_a = 0$ and $\Delta J = 0, \pm 1$ selection rules, where *J* is the quantum number associated with the total angular momentum exclusive of nuclear spin, and K_a is the quantum number associated with the projection of the total angular momentum onto the molecule's *A*-axis (corresponding to the $B^+ \cdots H_2$ bond). Altogether, 28 transitions were assigned to the $K_a = 1-1$ sub-band (P-branch 12 lines, Q-branch 3 lines, R-branch 13 lines), with asymmetry doublets resolved in the P and R branches. Transition wavenumbers and assignments are provided as Supporting Information.[28]

The $K_a = 1-1$ transitions were fitted using an *A*-reduced Watson asymmetric top Hamiltonian,[29] yielding the ground and excited state *B* and *C* rotational constants (related to the length of the $B^+ \cdots H_2$ bond), and the Δ_J centrifugal distortion constant (related to the stretching force constant of the $B^+ \cdots H_2$ bond). It is not possible to determine ground and excited state *A* rotational constants through analysis of the parallel *A*-type transition. Therefore, for the fit, A'' and A' were constrained to 59.33 and 56.37 cm^{-1}, the rotational constant of free H_2 in the $n_{HH} = 0$ and $n_{HH} = 1$ states, respectively.[30] Note that the fits are quite insensitive to the values of A'' and A'; virtually identical *B* and *C* constants are obtained for values of A'' and A' ranging from 50 to 60 cm^{-1}. Spectroscopic constants determined from the fit are listed in Table 1.

Table 1. Spectroscopic Constants for B^+-H_2 Obtained by Fitting the ν_{HH} $K_a = 1-1$ Transitions to a Watson *A*-Reduced Hamiltonian[a]

	exp		calc	
	$n_{HH} = 0$	$n_{HH} = 1$	CCSD(T)	MP2
B	1.9565(10)	2.0276(10)		
C	1.8498(10)	1.9045(10)		
$\bar{B}$	1.9032(10)	1.9660(10)		
$\Delta_J \times 10^4$	2.3(1)	2.3(1)		
ν_{sub}[b]	3936.11(1)			
ν_{HH}[c]	3940.6(1.5)		3975	3966
$\Delta\nu_{HH}$[c]	−220.6(1.5)		−186	−195
R_o/Å[d]	2.262	2.224		
R_e/Å[d]			2.25	2.27
ω_s	346	364	346	345
ω_b			504	511
D_0[e]	1330			1170

[a] Unless otherwise indicated, the units are inverse centimeters. For each value, the error in the last significant figure(s) is given in brackets. Calculated values are from CCSD(T)/aug-cc-pVTZ and MP2/aug-cc-pVTZ calculations.[21] [b] Sub-band origin for $K_a = 1-1$ transitions. [c] CCSD(T) and MP2 H−H stretch frequencies and frequency shifts are scaled by factors of 0.945 and 0.921, respectively. [d] The experimental intermolecular separations correspond to vibrationally averaged values (R_o) whereas the theoretical value corresponds to the equilibrium separation (R_e). Because of zero-point vibrational motion along the intermolecular coordinate R_o should slightly exceed R_e. [e] Experimental D_0 from ref 20.

A notable feature of the B^+-H_2 infrared spectrum is that only the $K_a = 1-1$ sub-band associated with complexes containing ortho H_2 molecules is observed, whereas the $K_a = 0-0$ sub-band associated with complexes containing para H_2 is absent. There are several reasons for the predominance of complexes containing ortho H_2. First, in normal hydrogen gas the ortho modification of H_2 (associated with molecules having odd rotational quantum number *j*) is three times more abundant than the para modification (associated with molecules having even *j*). Second, as suggested in previous investigations,[23,31] the B^+-H_2 complexes containing ortho H_2 are more strongly bound, essentially because an ortho $j = 1$ H_2 molecule is easier to orient in the electric field arising from the B^+ ion than a para $j = 0$ H_2 molecule. Furthermore, the free $j = 1$ H_2 has about 120 cm^{-1} more rotational energy than does free $j = 0$ H_2; this rotational energy is partially quenched in the complex

(26) Kendall, R. A., Jr.; Harrison, R. J. *J. Chem. Phys.* **1992**, *96*, 6796.
(27) Frisch, M. J.; et. al. *Gaussian 03*, revision D.01, 2005.
(28) Transition wavenumbers and assignments can be accessed in the Supporting Information.
(29) Watson, J. In *Vibration Spectra and Structure*; Durig, J., Ed.; Elsevier: Amsterdam, 1977; Vol. 6, p 1.
(30) Bragg, S. L.; Brault, J. W.; Smith, W. H. *Astrophys. J.* **1982**, *263*, 999–1004.
(31) Lovejoy, C.; Nelson, D.; Nesbitt, D. J. *J. Chem. Phys.* **1987**, *87*, 5621–5628.

Table 2. Experimental and Calculated Dissociation Energies (D_0), H−H Stretch Vibrational Frequency Shifts ($\Delta\nu_{HH}$), Intermolecular Separations (R_o and R_e) and H−H Bond Length Changes (Δr_{HH}) for Selected M^+-H_2 Clusters[a]

	D_0/cm $^{-1}$		$\Delta\nu_{HH}$/cm^{-1}		R_o/Å	R_e/Å	Δr_{HH}/Å	NBO	
species	expt	calc	expt	calc	expt	calc	calc	charge M	config
Li^+-H_2	1675[b]	1513	−108[f]	−113	2.056	2.015	0.009	+0.99	[He]
B^+-H_2	1330[c]	1170	−221	−195	2.262	2.272	0.014	+0.98	$[He]2s^2 2p^{0.2}$
Na^+-H_2	860[d]	680		−68		2.472	0.005	+1.00	[Ne]
Al^+-H_2	470[e]	370	−66[g]	−64	3.035	3.011	0.005	+1.00	$[Ne]3s^2$

[a] Calculated values were obtained at the MP2/aug-cc-pVTZ level. Also listed the metal cation charges and electronic configurations determined from NBO calculations. [b] From rovibrational calculations described in ref 34. [c] Reference 20. [d] Reference 35. [e] Reference 36. [f] Reference 23. [g] Reference 25.

leading to a relative stabilization of B^+-H_2 (ortho) relative to B^+-H_2 (para). Therefore, in the ion source, B^+-H_2 (para) complexes are rapidly converted to B^+-H_2 (ortho) complexes through exothermic ligand switching reactions.

Because $K_a = 0-0$ transitions are not observed in the spectrum, at this stage it is not possible to ascertain precisely the band center for the ν_{HH} transition. However, one can anticipate that the band center will lie between Δb and $2\Delta b$ higher in energy than the $K_a = 1-1$ sub-band center ($\Delta b \sim 3$ cm^{-1} is the difference in the H_2 rotational constant in the $n_{HH} = 0$ and $n_{HH} = 1$ states[30]). The lower limit (3939 cm^{-1}) is based on the B^+-H_2 complex being a rigid prolate rotor, whereas the upper limit (3942 cm^{-1}) corresponds to a complex with free internal rotation of the hydrogen subunit—the actual situation will lie some way between these two extremes. The average of the limiting values (3940.6 cm^{-1}) corresponds to a red-shift of −220.6 cm^{-1} with respect to the $Q_1(0)$ transition of the free H_2 molecule.[30]

4. Discussion

The spectroscopic data for B^+-H_2 can be interpreted to yield quantitative structural and vibrational information, which together with the dissociation energy measurement of Kemper et al.[20] should serve as solid benchmarks for ab initio calculations. Tables 1 and 2 summarize the calculated and spectroscopic data. Generally, the spectroscopic data confirm that B^+-H_2 is a weakly bound electrostatic complex as predicted by previous ab initio calculations and bond dissociation energy measurements.

Due primarily to the charge−quadrupole electrostatic interaction, the complex prefers a T-shaped configuration with the linear configuration lying 998 cm^{-1} higher in energy (according to the MP2/aug-cc-pVTZ calculations). Despite the considerable energetic barrier for internal rotation, the complex should exhibit a relatively large zero-point bending excursion because of the H_2 molecule's large rotational constant. As previously pointed out, the main consequence of this, insofar as the spectroscopic constants are concerned, is that $B - C$ is larger than it would be for a rigid T-shaped molecule (that is, there is large asymmetry splitting).[23,31] Note that even under these circumstances the vibrationally averaged intermolecular separation (R_o) can be estimated from $\bar{B} = (B + C)/2$.

The vibrationally averaged $B^+ \cdots H_2$ intermolecular separation estimated from $\bar{B}$ ($R_o = 2.26$ Å) is close to the equilibrium separation determined from the CCSD(T)/aug-cc-pVTZ and MP2/aug-cc-pVTZ calculations of Sharp and Gellene ($R_e = 2.25$ and 2.27 Å, respectively).[21] Because of zero-point vibrational motion in the intermolecular stretching coordinate, one might expect R_o to be slightly larger than R_e. The similarity of the experimental R_o and computed R_e values may indicate that the existing calculations slightly overestimate the equilibrium intermolecular bond length. Ultimately, the best way of establishing contact between theory and experiment is through rovibrational calculations using a full three-dimensional potential energy surface, as has been accomplished for the Al^+-H_2 complex.[25]

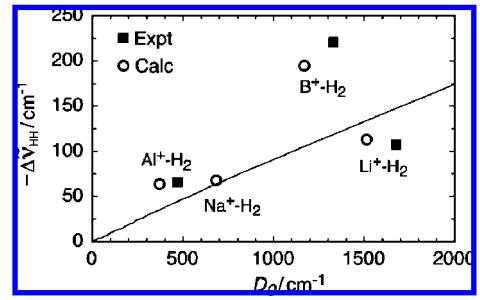

Figure 3. H−H stretch vibrational frequency shift ($-\Delta\nu_{HH}$) plotted against dissociation energy (D_0) for Li^+-H_2, B^+-H_2, Na^+-H_2, and Al^+-H_2. Both experimental and calculated values are shown. The line shows the predicted relationship between vibrational red-shift and dissociation energy for a point positive charge interacting with an H_2 molecule.[32,33]

Excitation of the H−H stretch mode leads to a slight shortening of the intermolecular bond (by 0.04 Å), which may be a consequence of the enhanced charge−quadrupole electrostatic interaction resulting from a ∼10% increase in the vibrationally averaged quadrupole moment of the H_2 molecule.[32] It is not possible to deduce the H−H bond length from the B and C rotational constants. However, on the basis of the MP2/aug-cc-pVTZ calculations, the H−H bond is predicted to be 0.014 Å longer than for the free H_2 molecule (the CCSD(T)/aug-cc-pVTZ calculations predict a 0.013 Å increase).[21] There is also excellent agreement between the experimental estimate for the intermolecular stretch mode determined from Δ_J and $\bar{B}$ and the calculated value (346 cm^{-1}, Table 1).

An exceptional attribute of the B^+-H_2 complex is the relatively large frequency shift for the H−H stretch mode ($\Delta\nu_{HH} = -220.6$ cm^{-1}) given its modest dissociation energy ($D_0 = 1330$ cm^{-1}). Generally, for dihydrogen complexes, the dissociation energy and the magnitude of the vibrational red-shift are strongly correlated.[5,33] The unusual nature of B^+-H_2 is apparent from Figure 3 where the $-\Delta\nu_{HH}$ is plotted against binding energy for Li^+-H_2, B^+-H_2, Na^+-H_2, and Al^+-H_2. Most noticeably, the B^+-H_2 complex has a smaller dissociation energy than Li^+-H_2 (1330 vs 1675 cm^{-1}) and a longer intermolecular bond (2.26 vs 2.06 Å), yet the frequency shift of the H−H stretch mode for B^+-H_2 (−221 cm^{-1}) is more than twice that of Li^+-H_2 (−108 cm^{-1}).[20,23,34] For Li^+-H_2 and Na^+-H_2, the relationship between the vibrational red-shift

(32) Hunt, J. L.; Poll, J. D.; Wolniewicz, L. *Can. J. Phys.* **1984**, *62*, 1719–23.
(33) Olkhov, R. V.; Nizkorodov, S. A.; Dopfer, O. *J. Chem. Phys.* **1997**, *107*, 8229–8238.
(34) Kraemer, W. P.; Špirko, V. *Chem. Phys.* **2006**, *330*, 190–203.

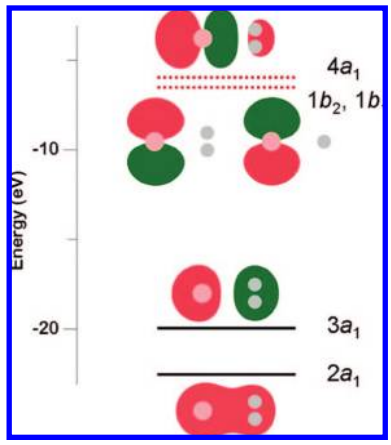

Figure 4. Molecular orbital diagram for the B^+-H_2 complex. Occupied MOs are indicated by solid lines, whereas unoccupied MOs are indicated by dotted lines.

and binding energy is compatible with predictions based on consideration of the electrostatic and induction interactions between H_2 and a point charge (solid line in Figure 3).[32,33] This is obviously not the case for B^+-H_2 (and to some extent Al^+-H_2) where the red-shift is clearly larger than expected from purely electrostatic and induction influences.

To rationalize the larger than expected vibrational red-shift for B^+-H_2 it is instructive to consider the valence molecular orbitals (MOs). As shown in Figure 4, the two occupied valence MOs can be considered as superpositions of the H_2 σ_g bonding orbital and the B^+ 2s orbital. The lower of the two, a bonding combination with respect to the intermolecular bond, has more 2s character, whereas the highest occupied molecular orbital (HOMO), which is an antibonding combination with respect to the intermolecular bond, has more σ_g character. Importantly, the HOMO also has a significant admixture of the B^+ $2p_z$ orbital such that the amplitude of the MO is diminished in the intermolecular region and enhanced on the opposite side of the B^+ atom. The net effect of this $2s/2p_z$ hybridization on the B^+ ion is that electron density is transferred from the H_2 σ_g orbital to the opposite side of the B^+ ion resulting in a weakening of the H−H bond (and consequently a large vibrational red shift). A similar although less pronounced effect occurs for Al^+-H_2, which has a comparable vibrational red-shift to Na^+-H_2, but a somewhat lower binding energy (see Figure 3). The Al^+ 3s orbital forms bonding and antibonding combinations with the H_2 σ_g orbital with the HOMO having some $3p_z$ character. The effect is weaker for Al^+-H_2 than for B^+-H_2 because of the Al^+ ion's larger valence radius (which also decreases the intermolecular bond strength). In contrast, for the Li^+-H_2 and Na^+-H_2 complexes, the unoccupied valence s and p orbitals lie well above the H_2 σ_g orbital and play little role in the intermolecular bonding.

The MO considerations outlined above are supported by a natural population analysis.[37] Results for B^+-H_2, Li^+-H_2, Na^+-H_2, and Al^+-H_2 are summarized in Table 2. For B^+-H_2, the B^+ atom was found to have a charge of +0.98 and an effective $[He]2s^2 2p_z^{0.2}$ configuration. Electron donation to the B^+ atom's $2p_z$ orbital occurs predominately from the H_2 σ_g bonding orbital, consistent with the large ν_{HH} red shift. In contrast, significantly less electron donation is found for Li^+-H_2, Na^+-H_2, and Al^+-H_2 (see Table 2). The appreciable electron donation from the H_2 σ_g bonding orbital to the B^+ atom's $2p_z$ orbital in B^+-H_2 is also consistent with the significant 0.014 Å lengthening of the H−H bond (compared to the free H_2 molecule), which is substantially greater than for Li^+-H_2 (0.009 Å), Na^+-H_2 (0.005 Å), and Al^+-H_2 (0.005 Å).

The current study implicates hybridization of the B^+ ion's 2s and $2p_z$ orbitals in the unusually large vibrational red-shift for the B^+-H_2 complex. Hybridization of a metal atom cation's half-filled or filled valence s orbital induced through polarization by an attached ligand was originally proposed to explain the properties of M^+-H_2 and M^+-CH_4 complexes.[38−40] The molecular ligand essentially pushes electron density to the opposite side of the atomic cation thereby mitigating the Pauli repulsion between the ligand and the s orbital. A further consequence is that complexes such as $B^+-(H_2)_2$, $Al^+-(H_2)_2$, $Mg^+-(H_2)_2$, $Mn^+-(H_2)_2$, and $Zn^+-(H_2)_2$ are predicted to have a bent structure because in this configuration the two ligands can concertedly polarize the metal cation core.[20,36,38,40] In contrast, complexes such as $Li^+-(H_2)_2$ and $Na^+-(H_2)_2$, which possess M^+ cores that are not easily polarized, are predicted to have structures in which the hydrogen molecules are on opposite sides of the metal cation core so that ligand−ligand repulsion is minimized.[23,38]

Finally, it is worth commenting on the vibrationally induced breakup of the B^+-H_2 complex. The experimental strategy relies on the excitation of metastable B^+-H_2 ($n_{HH} = 1$) resonances that result in $B^+ + H_2$ fragments. An estimate for the metastable state lifetime can be obtained through the uncertainty principle from the transition linewidths, which are on the order of 0.1 cm^{-1}. Taking the 0.017 cm^{-1} bandwidth of the infrared light source into account, the lifetime broadening contribution is estimated as ~0.05 cm^{-1}. This corresponds to a lifetime of 100 ps or 1.3×10^4 oscillations of the H_2 subunit. This lifetime should be taken as a provisional lower limit due to possible power broadening of the transitions.

5. Concluding Remarks

In conclusion we have obtained the first infrared spectrum of the B^+-H_2 complex, providing fundamental structural and vibrational data that can be used to test and refine computational approaches for describing the attachment of dihydrogen to boron ions and boron-containing materials.

The main outcomes of this work can be summarized as follows:

1. The B^+-H_2 complex possesses a rotationally resolved H−H stretch band red-shifted by 220.6 ± 1.5 cm^{-1} from the stretch fundamental of the free H_2 diatomic molecule.

2. The complex has a T-shaped equilibrium structure with an average intermolecular $B^+ \cdot \cdot \cdot H_2$ separation of 2.26 Å, decreasing by 0.04 Å when the H_2 subunit is vibrationally excited.

3. A 100 ps lower limit for the predissociation lifetime for B^+-H_2 ($n_{HH} = 1$) is estimated from the line broadening.

(35) Bushnell, J. E.; Kemper, P. R.; Bowers, M. T. *J. Phys. Chem.* **1994**, *98*, 2044–2049.
(36) Kemper, P. R.; Bushnell, J.; Bowers, M. T.; Gellene, G. I. *J. Phys. Chem.* **1998**, *102*, 8590–8597.
(37) Glendening, E. D.; Reed, A. E.; Carpenter, J. E.; Weinhold, F. *NBO*, version 3.1.
(38) Bauschlicher, C. W.; Partridge, H.; Langhoff, S. R. *J. Phys. Chem.* **1992**, *96*, 2475–2479.
(39) Bauschlicher, C. W.; Sodupe, M. *Chem. Phys. Lett.* **1993**, *214*, 489.
(40) Weis, P.; Kemper, P. R.; Bowers, M. T. *J. Phys. Chem. A* **1997**, *101*, 2809–2816.

4. The unusually large vibrational red-shift for the H−H stretch mode of B^+-H_2 (220.6 ± 1.5 cm^{-1}) is explained as due to electron donation from the H_2 σ_g bonding orbital to the empty B^+ $2p_z$ orbital. This orbital effect augments the familiar electrostatic and induction causes for the H−H red shift which operate for complexes such as Li^+-H_2 and Na^+-H_2.

Ideally, the studies of the electrostatic B^+-H_2 complex described in this paper will be complemented by spectroscopic investigations of the yet uncharacterized BH_2^+ molecular cation. Due to the large binding energy of BH_2^+, infrared photodissociation studies in which the fragment B^+ cation is detected are not feasible. Instead, it may be possible to probe the BH_2^+-Ar species by monitoring the argon atom loss channel; unfortunately this strategy involves sacrificing the prospect of obtaining a rotationally resolved spectrum of the bare BH_2^+ ion. Alternatively, it may be feasible to probe the species directly using conventional infrared absorption in a plasma discharge.

Ultimately, a comprehensive understanding of the BH_2^+/B^+-H_2 system will be derived from more extensive theoretical studies. Existing ab initio investigations have focused on stationary points of the potential energy surface. The future challenge is to develop potential energy surfaces describing the BH_2^+/B^+-H_2 system and to use these for computations of the rovibrational energy levels. Such studies will yield theoretical data directly comparable with the spectroscopic data reported in this work, deliver more reliable values for vibrational frequencies, give more accurate values for the dissociation energy by accounting properly for zero-point vibrational energy, and provide insights into rearrangement processes connecting the BH_2^+ and B^+-H_2 configurations.

Acknowledgment. The authors are grateful to the Australian Research Council and the University of Melbourne for financial support.

Supporting Information Available: Transition wavenumbers and assignments. This material is available free of charge via the Internet at http://pubs.acs.org.

JA8018302